

Parapositronium can decay into three photons

Andrzej Pokraka* and Andrzej Czarnecki†

Department of Physics, University of Alberta, Edmonton, Alberta, Canada T6G 2E1

We calculate the decay rate and spectrum for the decay of parapositronium into three photons. This process violates charge conjugation symmetry. It is forbidden within quantum electrodynamics but proceeds through the weak interaction. The branching ratio we find is fifty orders of magnitude smaller than the previous estimate.

PACS numbers: 31.15.ac, 36.10.Dr, 31.30.J-, 02.70.-c

I. INTRODUCTION

We compute the rate and photon energy spectrum of parapositronium (p-Ps) decaying into three photons ($\text{p-Ps} \rightarrow 3\gamma$). This decay violates charge conjugation symmetry (C -symmetry) and cannot happen in pure quantum electrodynamics (QED); weak interactions must be included.

Since this decay violates C -symmetry, it must also violate parity in order to conserve CP . Thus, the final state is composed of three spatially symmetric photons with vanishing total angular momentum. This final state is identical to that of the neutral pion decay to three photons ($\pi^0 \rightarrow 3\gamma$) [1].

Like the decay of ortho-positronium (o-Ps) into a photon and a neutrino-antineutrino pair ($\text{o-Ps} \rightarrow \gamma\nu_\ell\bar{\nu}_\ell$), the $\text{p-Ps} \rightarrow 3\gamma$ and $\pi^0 \rightarrow 3\gamma$ decays must contain an axial-vector interaction in the trace along the fermion line in order to break C -symmetry [1, 2]. At the one-loop level, this restricts the relevant diagrams to those that do not contain virtual photons.

Our result corrects the previous estimate, [3], by 50 orders of magnitude. While this correction does not influence the prospect of detecting $\text{p-Ps} \rightarrow 3\gamma$, it is a signal that also the related $\pi^0 \rightarrow 3\gamma$ decay may be more suppressed than previously thought. This is important because there have been experimental searches for the $\pi^0 \rightarrow 3\gamma$ decay [4].

In Sec. II we calculate the total amplitude to order $\mathcal{O}(m_e^4/m_W^4)$ where m_e is the mass of the electron and m_W is the mass of the W -boson. In Sec. III we use the result of Sec. II to compute the decay rate, branching ratio and photon spectrum of $\text{p-Ps} \rightarrow 3\gamma$ decays. We conclude in Sec. IV.

II. DECAY AMPLITUDE

To study the $\text{p-Ps} \rightarrow 3\gamma$ decay, it is convenient to write the amplitude as a sum of tensors made up of the external momentum multiplied by scalar functions, F_i , called form factors. The form factors are functions of the only available scalars: x, y, z where $x, y, z = k_{1,2,3}^0/m_e$ and k_i is the 4-momentum of the i^{th} photon in the final state. Gauge invariance of the photon field and Bose symmetry place restrictions on the form factors.

The construction of the $\text{p-Ps} \rightarrow 3\gamma$ decay amplitude is the same as for the $\pi^0 \rightarrow 3\gamma$ decay [1] (detailed in Appendix A). The amplitude is given by

$$\mathcal{M} = \epsilon_{\mu_1}^* \epsilon_{\mu_2}^* \epsilon_{\mu_3}^* \mathcal{M}^{\mu_1\mu_2\mu_3}(k_1, k_2, k_3) \quad (1)$$

where

$$\begin{aligned} \mathcal{M}^{\mu_1\mu_2\mu_3}(k_1, k_2, k_3) = & \left(k_1^{\mu_3} - k_2^{\mu_3} \frac{k_1 \cdot k_3}{k_2 \cdot k_3} \right) (k_1^{\mu_2} k_2^{\mu_1} - k_1 \cdot k_2 g^{\mu_2\mu_1}) F_1(x, y, z) \\ & + \left(k_1^{\mu_2} - k_3^{\mu_2} \frac{k_1 \cdot k_2}{k_2 \cdot k_3} \right) (k_3^{\mu_1} k_1^{\mu_3} - k_3 \cdot k_1 g^{\mu_1\mu_3}) F_2(x, y, z) \\ & + \left(k_2^{\mu_1} - k_3^{\mu_1} \frac{k_1 \cdot k_2}{k_1 \cdot k_3} \right) (k_3^{\mu_2} k_2^{\mu_3} - k_2 \cdot k_3 g^{\mu_2\mu_3}) F_3(x, y, z) \\ & + [k_2^{\mu_3} (k_1^{\mu_2} k_3^{\mu_1} - k_1 \cdot k_3 g^{\mu_2\mu_1}) - k_1^{\mu_3} (k_3^{\mu_2} k_2^{\mu_1} - k_3 \cdot k_2 g^{\mu_2\mu_1}) \\ & \quad + k_2^{\mu_1} k_1 \cdot k_3 g^{\mu_3\mu_2} + k_3^{\mu_2} k_1 \cdot k_2 g^{\mu_3\mu_1} - k_1^{\mu_2} k_2 \cdot k_3 g^{\mu_3\mu_1} - k_3^{\mu_1} k_1 \cdot k_2 g^{\mu_3\mu_2}] F_4(x, y, z). \end{aligned} \quad (2)$$

* pokraka@ualberta.ca

† andrzejc@ualberta.ca

and the ϵ_i are the photon polarizations.

Bose symmetry places restrictions on the form factors such that only F_1 and F_4 need to be calculated [1],

$$F_2(x, y, z) = F_1(z, y, x), \quad (3)$$

$$F_3(x, y, z) = F_1(z, x, y). \quad (4)$$

The form factors F_1 and F_4 can be projected out from the total amplitude by contracting the total amplitude with suitable tensors (Appendix A).

To lowest order in perturbation theory, $p\text{-Ps} \rightarrow 3\gamma$ proceeds through one-loop processes in electroweak theory. In the non-linear renormalizable gauge (R_ξ)

$$\begin{aligned} \mathcal{L}_{\text{Gauge-fix}} = & -\frac{1}{2\alpha}(\partial^\mu A_\mu)^2 - \frac{1}{2\eta}(\partial^\mu Z_\mu - \eta m_Z \chi)^2 \\ & - \frac{1}{\xi}(\partial^\mu W_\mu^+ - i\xi m_W \phi^+ - ig A_\mu^3 W^{+\mu})(\partial^\mu W_\mu^- + i\xi m_W \phi^- + ig A_\mu^3 W^{-\mu}), \end{aligned} \quad (5)$$

where ξ is the W -boson gauge parameter, the three point Goldstone- W -photon vertex disappears, reducing the number of diagrams that need to be computed [5, 6]. This makes this gauge a convenient choice for our problem. The Feynman rules in this gauge are listed in Appendix B.

To calculate the amplitude the electron and positron are approximated to be at rest with momentum $p = (m, \mathbf{0})$. The $p\text{-Ps}$ projection operator $\Psi_{p\text{-Ps}} = (1 + \gamma^0)\gamma^5/2\sqrt{2}$ [7] is used to project out the correct spin configuration of the electron and positron.

The classes of diagrams that contribute to $p\text{-Ps} \rightarrow 3\gamma$ decays are restricted to those that break C -symmetry (i.e., contain a single axial interaction in the fermion line). Furthermore, diagrams containing virtual Z -bosons are suppressed by $1 - 4 \sin^2 \theta_W$ vector coupling to the electrons (where θ_W is the weak mixing angle and $\sin^2 \theta_W \approx 0.238$ is numerically close to $1/4$ [8]) or by the mass of heavier charged particles in a loop. We therefore ignore all diagrams containing Z -bosons.

The diagrams that we consider are collected in Fig. 1. Counterterm diagrams 1(g) and 1(h) (Appendix C) cancel the divergences of Figs. 1(e) and 1(f).

As a consistency check, we keep the gauge parameter of the W -bosons and show that the form factors in the total amplitude are gauge independent. Namely,

$$F_i(x, y, z = 2 - x - y) = \frac{14G_F^2 e^3 m_e}{720\pi^2 m_W^4} (1 - x) f_i(x, y) \quad (6)$$

where

$$f_1 = \frac{1 - y}{x} - \frac{1 - x}{y}, \quad (7)$$

$$f_2 = (1 - y) \left(\frac{1}{2 - x - y} - \frac{1}{x} \right), \quad (8)$$

$$f_3 = (1 - y) \left(\frac{1}{2 - x - y} - \frac{1}{y} \right), \quad (9)$$

$$f_4 = 0. \quad (10)$$

Here, $G_F \simeq 1.166 \cdot 10^{-5}/\text{GeV}^2$ is the Fermi coupling constant [9] and $e > 0$ is the electric charge of a proton. Substituting these form factors into (2) yields the total amplitude. The form factors (7)-(10) have corrections of order $\mathcal{O}(m_e^2/m_W^2)$ that we ignore. Their leading order terms are remarkably simple compared to the one-loop form factors for the analogous decay of o-Ps [10]. This is because the W -loop is essentially point like relative to the other distance scale in Ps.

III. DECAY RATE AND PHOTON SPECTRUM

With the results of the previous section, it is simple to obtain the decay rate and photon spectrum. Using (2) with (6), we obtain

$$\Gamma(p\text{-Ps} \rightarrow 3\gamma) = \frac{(14700\pi^2 - 145081)G_F^2 \alpha^6 m_e^{13}}{58320000\pi^5 m_W^8} \approx 3.5 \cdot 10^{-67} \text{s}^{-1}. \quad (11)$$

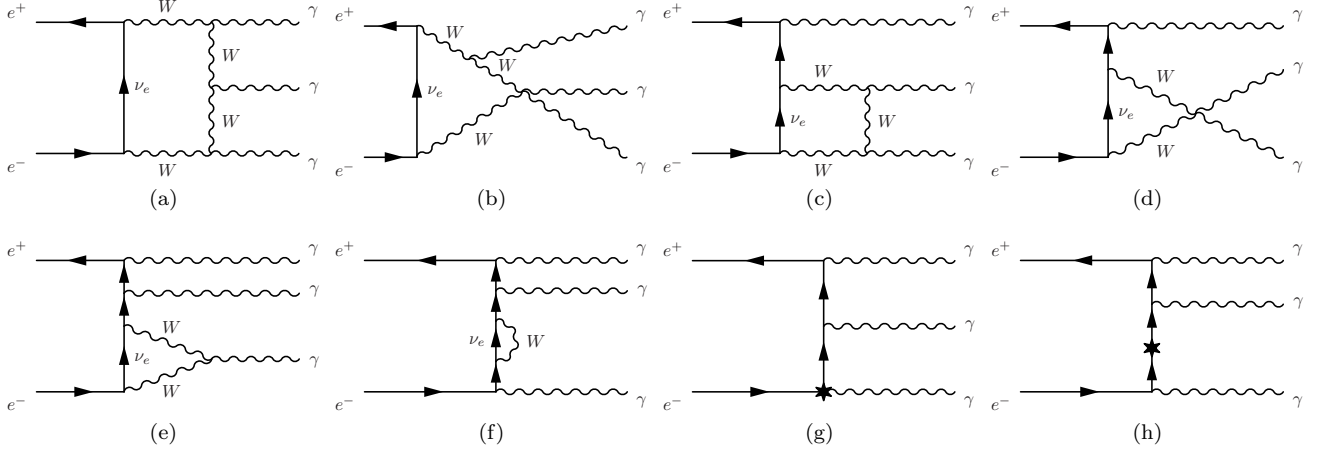


FIG. 1. The dominant contributions to the C -violating amplitude of $p\text{-Ps} \rightarrow 3\gamma$. In addition to Figs. (a)-(f) there are the analogous diagrams where the W -bosons are replaced by charged Goldstone bosons ϕ^\pm . Figs. (g) and (h), are counterterm diagrams that remove the divergences of Figs. (e) and (f).

The corresponding branching ratio is

$$\text{Br}(p\text{-Ps} \rightarrow 3\gamma) = \frac{\Gamma(p\text{-Ps} \rightarrow 3\gamma)}{\Gamma(p\text{-Ps} \rightarrow 2\gamma)} \approx 4.4 \cdot 10^{-77}. \quad (12)$$

Comparing with the estimated branching ratio of [3],

$$\alpha [G_F m_e^2 (1 - 4 \sin^2 \theta_W)]^2 \approx 10^{-27}, \quad (13)$$

we see that the decay rate was overestimated. Additionally, the contribution we find is not suppressed by $1 - 4 \sin^2 \theta_W$ whose presence was assumed in [3].

Through direct calculation, we observe suppression of the $p\text{-Ps} \rightarrow 3\gamma$ decay relative to the estimate [3]. Our qualitative understanding is as follows. Consider the annihilation of e^-e^+ at high energies (centre of mass energies greater than about 1 GeV). In this energy regime, the mass of the electron/positron may be ignored and mass of the W -boson becomes the only relevant mass scale. Photon gauge invariance requires three powers of k_i in the amplitude, each of which must be divided by the only available mass: m_W . When transitioning from the high energy to the low energy regime, the W -boson mass dividing the k_i 's in the amplitude cannot be replaced by the electron mass. Of course, in a low energy process, the electron mass becomes important and may give rise to additional contributions, but they will be no less suppressed by the W -boson mass. We believe that an analogous suppression by the eight powers of the W -boson mass may affect other C -violating decays, for example $\pi^0 \rightarrow 3\gamma$. We think that this has been overlooked in previous studies like [1]. However, a detailed determination of meson decays is beyond the scope of this paper.

The corresponding photon spectrum is calculated to be

$$\frac{1}{\Gamma} \frac{d\Gamma}{dx} = \frac{70(1-x)}{14700\pi^2 - 145081} \left[-840 + 7700x^2 - 14560x^3 + 10192x^4 - 2489x^5 - \frac{840(2+6x-6x^2+x^3)(1-x)^4 \ln(1-x)}{(2-x)x} \right] \quad (14)$$

where x is the energy of one of the photons divided by the electron mass and $\Gamma = \Gamma(p\text{-Ps} \rightarrow 3\gamma)$ is given in (11). Equation (14) is plotted in Fig. 2.

When one photon has maximal energy ($x = 1$), the other two photons must move collinearly and in the opposite direction. However, this configuration does not conserve angular momentum and thus the photon spectrum (14) vanishes at $x = 1$. This is in contrast with the spectrum of the orthopositronium decay into 3γ , which reaches its maximum at $x = 1$. Fig. 2 also shows the suppression of low-energy photon emission by a neutral system. In the low energy limit the photon spectrum is of $\mathcal{O}(x^5)$ in agreement with Low's theorem [11].

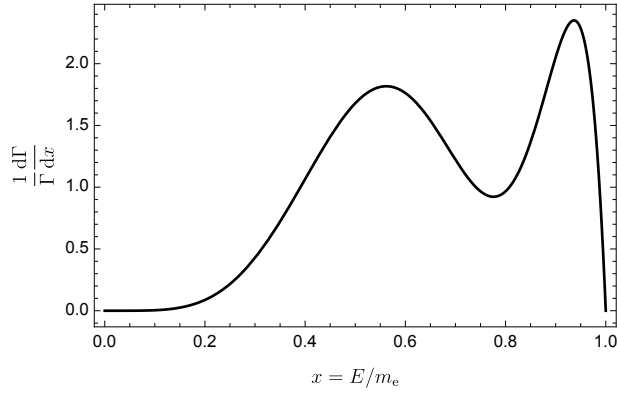


FIG. 2. Plot of the p-Ps $\rightarrow 3\gamma$ Photon spectrum (14). Here, $x = E/m_e$ is the energy of a photon, E , divided by the electron mass.

IV. CONCLUSIONS

We have presented the first calculation of the decay of parapositronium into an odd number of photons. The fact that we correct the previous estimate by 50 orders of magnitude signals that analogous meson decays should be reanalyzed. This is especially warranted in view of ongoing experimental searches for analogous C -violating pseudoscalar meson decays [12–15].

Positronium has been used to test C -symmetry by looking for forbidden QED decay modes such as p-Ps $\rightarrow 3\gamma$ and o-Ps $\rightarrow 4\gamma$ [16–18]. Our calculation demonstrates that standard model contributions to p-Ps $\rightarrow 3\gamma$ decays are far smaller than conceivable experimental sensitivities. Any detection of p-Ps $\rightarrow 3\gamma$, in the near future would be a signal of new physics [19, 20].

ACKNOWLEDGMENTS

This research was supported by the Natural Sciences and Engineering Research Council of Canada (NSERC).

[1] D. A. Dicus, Phys. Rev. **D12**, 2133 (1975).
[2] A. Pokraka and A. Czarnecki, Phys. Rev. **D94**, 113012 (2016), 1611.07645.
[3] W. Bernreuther and O. Nachtmann, Z. Phys. **C11**, 235 (1981).
[4] J. McDonough *et al.*, Phys. Rev. **D38**, 2121 (1988).
[5] K. Fujikawa, Phys. Rev. **D7**, 393 (1973).
[6] M. B. Gavela, G. Girardi, C. Malleville, and P. Sorba, Nucl. Phys. **B193**, 257 (1981).
[7] A. Czarnecki, K. Melnikov, and A. Yelkhovsky, Phys. Rev. **A59**, 4316 (1999), hep-ph/9901394.
[8] A. Czarnecki and W. J. Marciano, Nature **435**, 437 (2005).
[9] W. J. Marciano, Phys. Rev. **D60**, 093006 (1999), hep-ph/9903451.
[10] G. S. Adkins, D. R. Drost, D. Rastawicki, and R. N. Fell, Phys. Rev. A **81**, 042507 (2010).
[11] F. E. Low, Phys. Rev. **110**, 974 (1958).
[12] E391a, Y. C. Tung *et al.*, Phys. Rev. **D83**, 031101 (2011), 1011.4403.
[13] S.-Y. Ho and J. Tandean, Phys. Rev. **D82**, 114010 (2010), 1007.4496.
[14] B. M. K. Nefkens *et al.*, Phys. Rev. **C72**, 035212 (2005).
[15] KLOE, A. Aloisio *et al.*, Phys. Lett. **B591**, 49 (2004), hep-ex/0402011.
[16] P. Moskal *et al.*, Acta Phys. Polon. **B47**, 509 (2016), 1602.05226.
[17] S. N. Glinenko, N. V. Krasnikov, V. A. Matveev, and A. Rubbia, Phys. Part. Nucl. **37**, 321 (2006).
[18] A. P. Mills and S. Berko, Phys. Rev. Lett. **18**, 420 (1967).
[19] M. Caravati, A. Devoto, and W. W. Repko, Phys. Lett. **B556**, 123 (2003), hep-ph/0211463.
[20] H. Grosse and Y. Liao, Phys. Lett. **B520**, 63 (2001), hep-ph/0104260.
[21] A. Denner, Fortsch. Phys. **41**, 307 (1993), 0709.1075.
[22] W. Hollik, Adv. Ser. Direct. High Energy Phys. **14**, 37 (1995).

Appendix A: Amplitude structure

This appendix summarizes the construction of the amplitude presented in [1]. We start by defining the matrix element for $p\text{-Ps} \rightarrow 3\gamma$ by

$$\mathcal{M}(k_1, k_2, k_3) = \epsilon_{\mu_1}^* \epsilon_{\mu_2}^* \epsilon_{\mu_3}^* \mathcal{M}^{\mu_1 \mu_2 \mu_3}(k_1, k_2, k_3) \quad (\text{A1})$$

where ϵ_i are the polarizations of the external photons. The most general third rank tensor constructed out of the external photon momentum contains 27 terms of the form $k_i^{\mu_1} k_j^{\mu_2} k_k^{\mu_3}$, 9 terms of the form $k_l^{\mu_i} g^{\mu_j \mu_k}$. Since the amplitude will be contracted with $\epsilon_{\mu_3}^* \epsilon_{\mu_2}^* \epsilon_{\mu_1}^*$ we can identify $k_i^{\mu_i} = 0$. This reduces the number of terms to 14 possible terms: 8 of the type $k_i^{\mu_1} k_j^{\mu_2} k_k^{\mu_3}$ and 6 of the type $k_l^{\mu_i} g^{\mu_j \mu_k}$. Gauge invariance,

$$k_{3\mu_3} \mathcal{M}^{\mu_3 \mu_2 \mu_1} = k_{2\mu_2} \mathcal{M}^{\mu_3 \mu_2 \mu_1} = k_{1\mu_1} \mathcal{M}^{\mu_3 \mu_2 \mu_1} = 0, \quad (\text{A2})$$

then restricts the structure of the amplitude to that of equation (2).

To project out the form factors we need the projection tensors. The F_1 projector is obtained by setting

$$F_1 = -\frac{k_2 \cdot k_3}{2(k_1 \cdot k_3)(k_1 \cdot k_2)^3} \quad (\text{A3})$$

$$F_2 = F_3 = 0 \quad (\text{A4})$$

$$F_4 = -\frac{1}{4(k_1 \cdot k_3)(k_1 \cdot k_2)^2} \quad (\text{A5})$$

in equation (2). Similarly, setting

$$F_1 = -\frac{1}{(k_1 \cdot k_3)(k_1 \cdot k_2)^2} \quad (\text{A6})$$

$$F_2 = \frac{1}{4(k_1 \cdot k_3)^2(k_1 \cdot k_2)} \quad (\text{A7})$$

$$F_3 = -\frac{1}{4(k_2 \cdot k_3)^2(k_1 \cdot k_2)} \quad (\text{A8})$$

$$F_4 = -\frac{1}{2(k_2 \cdot k_3)(k_1 \cdot k_3)(k_1 \cdot k_2)} \quad (\text{A9})$$

in equation (2) yields the F_4 projector.

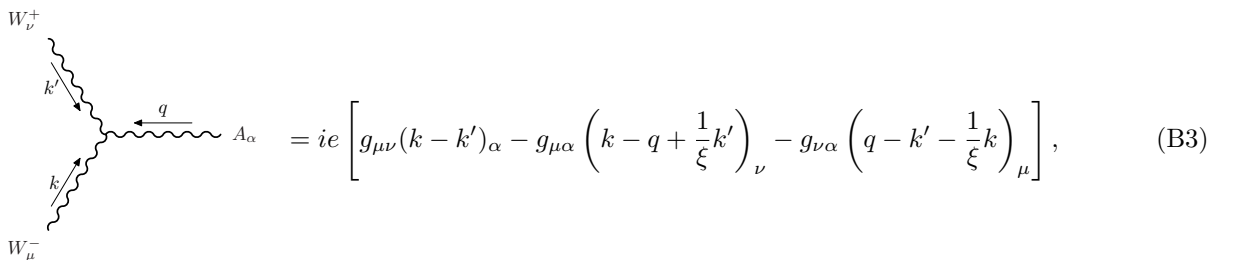
Appendix B: Feynman rules in the non-linear R_ξ gauge

In this appendix, we list the Feynman rules used in our calculation. The propagator for the W -boson and Goldstone boson propagators are unchanged from the linear R_ξ gauge and given by

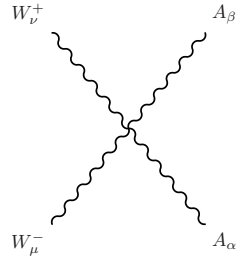
$$\mu \xrightarrow[W]{q} \nu = \frac{-i}{q^2 - m_W^2} \left(g^{\mu\nu} - (1 - \xi) \frac{q^\mu q^\nu}{q^2 - \xi m_W^2} \right) \quad (\text{B1})$$

$$\xrightarrow[\phi^-]{q} = \frac{i}{q^2 - \xi m_W^2} \quad (\text{B2})$$

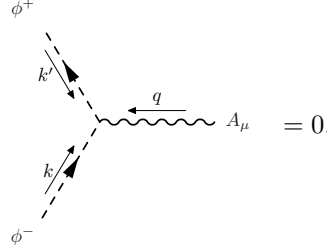
where ξ is the gauge parameter. Next we list the relevant vertices in the non-linear R_ξ gauge that differ from those in the linear R_ξ gauge:



$$W_\nu^+ \quad \text{---} \quad \text{---} \quad A_\alpha = ie \left[g_{\mu\nu} (k - k')_\alpha - g_{\mu\alpha} \left(k - q + \frac{1}{\xi} k' \right)_\nu - g_{\nu\alpha} \left(q - k' - \frac{1}{\xi} k \right)_\mu \right], \quad (\text{B3})$$

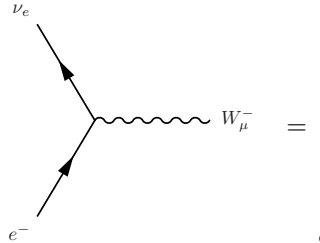


$$= -ie^2 \left[2g_{\mu\nu}g_{\alpha\beta} - \left(1 - \frac{1}{\xi}\right) (g_{\mu\alpha}g_{\nu\beta} + g_{\mu\beta}g_{\nu\alpha}) \right], \quad (\text{B4})$$

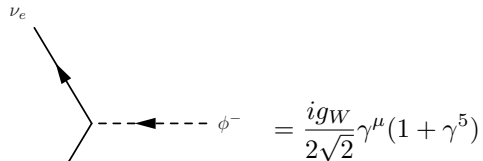


$$= 0. \quad (\text{B5})$$

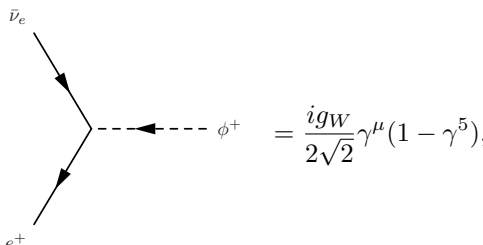
The remaining vertices are unchanged from those in the linear R_ξ gauge (consult Ref. [21] for a complete list of vertices in the linear R_ξ gauge):



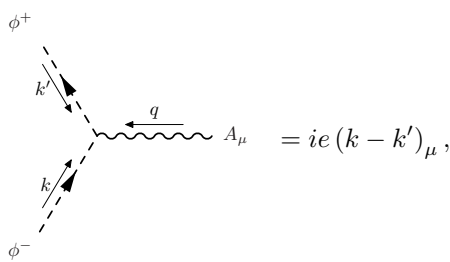
$$= \frac{ig_W}{2\sqrt{2}} \gamma^\mu (1 - \gamma^5), \quad (\text{B6})$$



$$= \frac{ig_W}{2\sqrt{2}} \gamma^\mu (1 + \gamma^5) \quad (\text{B7})$$



$$= \frac{ig_W}{2\sqrt{2}} \gamma^\mu (1 + \gamma^5), \quad (\text{B8})$$



$$= ie (k - k')_\mu, \quad (\text{B9})$$

$$= 2ie^2 g_{\mu\nu}. \quad (\text{B10})$$

Here, $g_W = e/\sin \theta_W$ is the weak coupling constant and $e > 0$ is the electric charge of a proton.

Appendix C: Renormalization

For our purposes, it is enough to limit our attention to axial contributions to the electron self energy and the renormalized $e^- e^+ \gamma$ vertex. The axial contributions to these quantities are [22]

$$\Sigma_A(\not{p}) = \not{p} \gamma^5 \left(\hat{\Sigma}_A(p^2) - \delta Z_A \right), \quad (\text{C1})$$

$$\Gamma_A^\mu = ie \delta Z_A \gamma^\mu \gamma^5. \quad (\text{C2})$$

Above, $\hat{\Sigma}_A$ is the axial part of the self energy not including the counterterm.

The counterterm contribution to the electron propagator and $e^- e^+ \gamma$ vertex is fully determined by the axial part of the electron field strength, δZ_A . Using on-shell renormalization conditions, the axial part of the electron field strength is $\delta Z_A = \hat{\Sigma}_A(\not{p} = m_e)$.